Article

J. Mex. Chem. Soc. **2008**, *52(1)*, 88-92

ISSN 1870-249X

Molecular Dynamics Simulations of the Solubility of H_2S and CO_2 in Water

Roberto López-Rendón,[1, 2] and José Alejandre[1*]

[1] Departamento de Química Universidad Autónoma Metropolitana-Iztapalapa Av. San Rafael Atlixco 186 09340, México D.F., México. jra@xanum.uam.mx

[2] Department of Computer Science and Engineering, University of Notre Dame, Notre Dame, IN 46556, USA

Recibido el 12 de octubre del 2007; aceptado el 14 de marzo del 2008

Abstract. We have performed molecular dynamics simulations at constant temperature and pressure to calculate the solubility of carbon dioxide (CO_2) and hydrogen sulfide (H_2S) in water. The solubility of gases in water is important in several technological problems, in particular in the petroleum industry. The calculated liquid densities as function of temperature are in good agreement with experimental data. The results at the liquid-vapor equilibrium show that at low temperatures there is an important amount of gases at the interface. The adsorption of gases in the liquid phase decreases as temperatures increases.
Key words: Molecular dynamics simulations, acid gases, solubility.

Resumen. Se desarrollaron simulaciones de dinámica molecular a temperatura y presión constante para obtener la solubilidad del dióxido de carbono (CO_2) y del ácido sulfhídrico (H_2S) en agua. La solubilidad de los gases en agua es importante en varios problemas tecnológicos, en particular en la industria del petróleo. Las densidades obtenidas en fase líquida a distintas temperaturas reproducen muy bien los datos experimentales. Los resultados en el equilibrio líquido-vapor muestran que hay una fuerte adsorción de gases en la interfase. La adsorción en la fase líquida disminuye con el aumento de la temperatura.
Palabras clave: Simulaciones de dinámica molecular, gases ácidos, solubilidad.

1 Introduction

The solubility of gases in mixed solvents is an important factor for the design, development and optimization of various industrial processes. Gas solubility data are also useful in providing essential information about thermodynamic and structural properties of solutions. The experimental determination of the solubility of gases in liquids for industrial systems is well known [1, 2]. These measurements are expensive because the conditions of pressure and temperature they are carried out. Nevertheless, it is necessary to understand the available experimental data and organize them over a wide range of temperatures and pressures to be used in the modeling of vapor-liquid equilibrium.

The two main reasons to investigate the thermodynamic properties of carbon dioxide water are the application to the oil and gas industry and CO_2 sequestration. Carbon dioxide and water are often found together in natural gas streams and also in oil reservoirs as part of enhanced oil recovery. The presence of carbon dioxide and water in these environments may cause complications such as corrosion and hydrate formation. On the other hand, various CO_2 sequestration schemes have generated significant interest in the thermodynamic properties of carbon dioxide-water systems. Besides, the issue of global climate change due to emissions of so-called greenhouse gases including carbon dioxide is of great importance to the future development of energy and power technology. It is for that reason that studies have been performed to remove carbon dioxide from natural or refinery gases. The CO_2 adsorption into a liquid agent is the most commonly used process for the bulk removal of CO_2. Accurate knowledge of the behavior of these systems over a wide range of pressures and temperatures is essential for industrial applications. In particular, reliable solubility data of carbon dioxide in water over a wide range of temperatures and pressures are necessary to develop and to validate especially adapted thermodynamic models.

Accurate knowledge of phase behavior in water-H_2S systems is crucial for designing and operation of pipelines and production/processing facilities as many sour reservoir fluids containing hydrogen sulfide and water. In general, it is desirable to avoid the formation of condensed water to reduce the risk of gas hydrate formation, ice formation, corrosion, and two-phase flow problems. On the other hand, oil and gas producers have been faced with a growing challenge to reduce atmospheric emissions of acid gases, including hydrogen sulfide, produced from sour hydrocarbon reservoirs, because of environmental regulations. When acid gases are extracted, one option of their disposal is by injection into an underground zone. As acid gases are normally saturated with water in gas treatment units, a comprehensive coverage of the many design considerations for acid gases disposal requires knowledge of the phase equilibrium in a water-hydrogen sulfide system.

An important issue in this area is to improve the accuracy of vapor-liquid equilibrium measurements of acid gases in water in conditions where the experimental techniques are difficult to use. This is an area where computer simulation methods can provide information at molecular level with greater detail than is experimentally accessible. The results obtained from this technique can be used to interpret experimental results and also to test more theoretical approaches. The simulation methods are powerful tools for the prediction of thermodynamic properties of mixtures from pure components data.

From molecular simulation point of view, the prediction of thermodynamical and structural properties requires the knowledge of a good interaction potential model. Several potential models have been proposed to simulate H_2S as a pure

component. Kristof and Liszi [3] developed a force field that contained four charged sites. The model accurately predicts the liquid-vapor phase diagram. Shyamal [12] proposed a new force field that contains three charged sites and is able to reproduce the experimental saturation densities. He used this model to study vapor-liquid phase equilibrium of H_2S with hydrocarbon chains. His results were in good agreement with available experimental data.

Regarding CO_2, Geiger *et al.* [4] studied the effect of intermolecular potential and interaction induced polarizability on the depolarized Rayleigh scattering in supercritical CO_2 by using molecular dynamics computer simulation. Murthy et. al [5] proposed simple force field models to describe the properties of carbon dioxide in different phases. One of the most important models used in the literature is that developed by Harris and Yung [10]. Their model accurately reproduces the experimental liquid-vapor coexisting densities. da Rocha and co-workers have reported results of the CO_2-water interface [6], as well as the surfactant CO_2-water interface [7]. Recently, Urukova *et al.* [8] reported the solubility of carbon dioxide in pure methanol, and in aqueous solutions of methanol by using the Gibbs ensemble Monte Carlo simulation method.

In this work we investigate the solubility of acid gases in water by molecular dynamics simulations. We show that the force fields used in this work are good enough to reproduce experimental data of CO_2 and H_2S as pure components and mixed with water.

The remainder of this work is organized as follows: The description of the potential models and calculated properties are given in Section 2. The simulation details are found in Section 3. In the Section 4 we discuss the simulation results of CO_2 and H_2S, both in liquid phase and in liquid-vapor equilibrium. A comparison with experimental data is also given. Finally the conclusions and references are given.

2 Force fields and calculated properties

The force fields used in this work were taken from the literature. Water is represented by the flexible SPC/E interaction model [9]. The parameters used for the intramolecular interactions are k_r = 557733.0 K Å^{-2} and for k_θ = 46067.4 K rad^{-2}. The equilibrium OH bond distances in water are fixed at a distance of 1 Å, with an HOH angle equal to 109.5 degrees. The model contains Coulombic interactions due to the three point charges located at the oxygen and hydrogen sites and a Lennard-Jones repulsion-dispersion interaction term as given in eq 1.1

$$U\left(r_{ij}\right)=\frac{1}{4\pi\varepsilon_0}\frac{q_i q_j}{r_{ij}}+4\varepsilon_{ij}\left[\left(\frac{\sigma_{ij}}{r_{ij}}\right)^{12}-\left(\frac{\sigma_{ij}}{r_{ij}}\right)^{6}\right], \qquad (1.1)$$

where q_i and q_j are the charges centered on the individual atoms of different water molecules, with a Lennard-Jones interaction only between oxygen atoms.

For the CO_2 we used the model of Harris et. al [10] called EPM2. This model was selected due to its simplicity and computational efficiency, as compared to more elaborated models such as those incorporating five point charges [11]. The model EPM2, consists of an electrostatic contribution due to three collinear partial charges located on the axis of symmetry of each O-C-O molecule at the positions with a fixed C-O bond length of 1.149 Å , plus three LJ terms, with a potential as in eq 1.1.

For the H_2S we use the model of Shyamal [12]. For this model, the optimum values for the H-S bonds and H-S-H angle are 1.365 and 91.5 degrees, respectively. The bond-stretching and bond-bending interaction energies were taken from the NERD force field model of alkanes. The nonbonded parameters and charges for each potential model are given in table 1. The molecular structure of CO_2 and H_2S are shown in Figure 1. The LJ parameters for the interactions between atoms in unlike molecules are calculated using the Lorentz-Berthelot combining rules given by eq. 1.2

$$\sigma_{ij}=\frac{\left(\sigma_{ii}+\sigma_{jj}\right)}{2} \text{ and } \varepsilon_{ij}=\left(\varepsilon_{ii}\varepsilon_{jj}\right)^{1/2}. \qquad (1.2)$$

The solubility of CO_2 and H_2S was calculated by using the molality of the solution

$$m_i(z)=\frac{\rho_i(z)}{M_i\rho_j(z)}, \qquad (1.3)$$

where $\rho_i(z)$ is the density profile in the liquid phase of component *i*. M_i and $\rho_j(z)$ are the molar mass and density profile for the component *j* respectively. In this work, the component *i* is CO_2 or H_2S and the component *j* is water.

The molecular density profile was obtained by

$$\left\langle\rho(z)\right\rangle=\frac{\left\langle N(z)\right\rangle}{A\Delta z}. \qquad (1.4)$$

Table 1. Lennard-Jones parameters and charges for water [9], CO_2 [10], and H_2S [12]

Site	CO_2	H_2S	Water	σ/Å	ε/k_B
O(CO_2)	-0.3256			3.033	80.507
C(CO_2)	0.6512			2.757	28.129
H(H_2S)		0.124		0.98	3.9
S(H_2S)		-0.248		3.72	250.0
H(H_2O)			0.4238	0.0	0.0
O(H_2O)			-0.8476	3.182	78.2

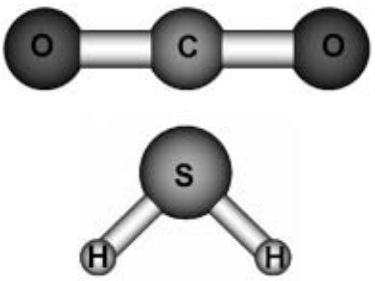

Fig. 1. Molecular structure of the acid gases. A) CO_2. b) H_2S. The bond lengths and bond angles are given in Section 2 and they have the same value in the liquid and interface simulations.

where $N(z)$ is the number of molecules in a slab located between z and $z + \Delta z$, $A = L_x L_y$ is the surface area and Δz is the width of the slab. In this work, Δz is 0.2 Å. The brackets denote time averaging.

3 Simulations details

Molecular dynamics simulations at constant temperature and and pressure were carried out to obtain the liquid density of CO_2 and H_2S as pure components at different temperatures as well as their solubility in water. A new integrator [13] which preserves the phase space volume was used with two Nosé-Hoover chains [14] coupled to the system: one to the particles and the other to the barostat. The method is based on a new approach applied to the original Martyna, Tobias, and Klein equations of motion [15]. The Lennard Jones and Coulomb interactions were handled by the Ewald sum [16] to properly evaluate the long range interactions. The cut-off distance Rc = 9.5 Å was used to calculate the real part of the potential and had the same value for all the simulations. The α parameter in the Ewald sums was 0.285 $Å^{-1}$ and 0.29 $Å^{-1}$ for the real part of the LJ and Coulomb potentials, respectively. The reciprocal part in both models was calculated using the Smooth Particle Mesh Ewald method [17]. The total number of molecules was 500 for all simulations in the liquid phase. The simulation box length was $L_x = L_y = L_z$ = 36.7238 Å. To make a direct comparison with experimental data, the external pressure in these simulations was 60.0 and 36.47 atm for CO_2 and H_2S, respectively. To simulate the liquid-vapor phase equilibrium of CO_2 and H_2S, we allocated 864 molecules in the center of a parallelepiped cell surrounded by vacuum. This is a common way of setting up the initial configuration when interfaces are being simulated. The dimensions of the simulation cell were $L_x = L_y$ = 37.8348 Å and L_z = 113.5 Å. The equilibrium was reached after 50000 time steps and the calculated properties were obtained by averaging 20 independent blocks of 10000. The calculated average temperature and pressure were the same as the impose values and not drift in the conserved quantity was observed. The simulations were performed using in-house developed molecular dynamics programs. The liquid phase simulations were carried out typically in 10 hours while the liquid-vapor simulations required around one week of CPU time in the supercomputer at UAM-Iztapalapa.

4 Results and Discussion

We report the density of CO_2 and H_2S as pure components in the liquid phase as a function of temperature and the solubility of them in water.

4.1 Pure components

As a first step in this investigation, we have performed molecular dynamics simulations at constant temperature and pressure to obtain the density as a function of temperature for the acid gases as pure components. The simulation results are compared with experimental data [19] and shown in Fig. 2. The force field used to simulate CO_2 and H_2S in this work gives results in excellent agreement with experimental data. The error in the calculation of these densities was less than 1%. The results for CO_2 are shown in Fig. 2-A where the external pressure was 60.0 atm, whereas the results for H_2S are shown in Fig. 2-B where the external pressure was 36.47 atm. The pressure and temperature calculated at the end of the simulations were the same as the external pressure and temperature applied to the system in both cases. These results suggest that we can use these force fields to study the solubility of CO_2 and H_2S in water.

4.2 Binary mixtures

In this work we study the vapor-liquid phase equilibrium of binary systems of H_2O-CO_2 and H_2O-H_2S. The density profiles were calculated using eq. 1.4 and are shown in Fig. 3 for both mixtures at two temperatures. The profiles have two interfaces with a liquid phase surrounded by vapor. The liquid phase contains water and acid gas while the vapor does not contain water.

The density profiles shown in Fig. 3-A, and Fig. 3-C are for H_2O-CO_2 system, whereas those in Fig. 3-B, and Fig. 3-D are for H_2O-H_2S. The density profiles in Fig. 3-A and Fig. 3-B are calculated at 313 K, whereas those in Fig. 3-C and in Fig. 3-D are at 450 K. The vapor pressure in both cases is around 1.1 MPa. It is observed that the concentration of CO_2 in the liquid phase is negligible, whereas that in the vapor phase is higher. There is an important amount of CO_2 at the interface. This finding suggests that the absorption of this gas is carried out at the interface and not in the liquid phase as considered experimentally. There is not experimental information, until our knowledge, about the amount of CO_2 at the interface. On the other hand, by using the same temperature and pressure for the H_2S, the simulation results show that its amount in the vapor phase is less than that of CO_2, whereas in the liquid phase the concentration is higher. Also a high concentration of H_2S is observed close to the interface, this acid gas has not

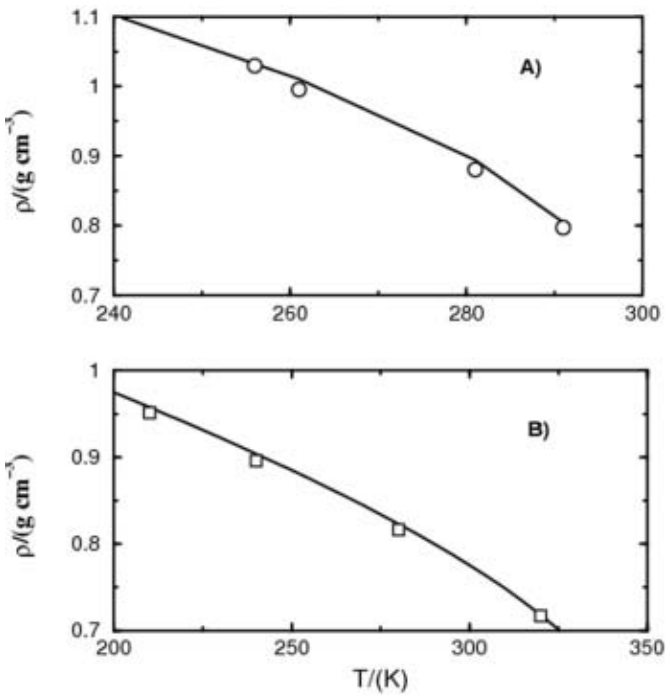

Fig. 2. Density as a function of temperature for acid gases. The solid lines are the experimental data and the symbols are the results from this work. A) CO_2. B) H_2S.

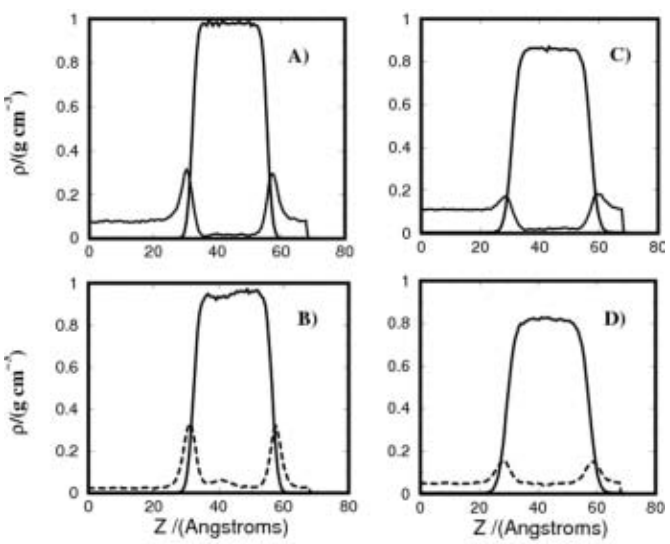

Fig. 3. Density profiles of acid gases in water. The top part is for CO_2 and the bottom part is for H_2S. The density profiles shown in A) and C) are at 313 K, whereas those of C) and D) are at 450 K, respectively.

either been measured in this region by any experimental method. The density of the water for this temperature is slightly lower than 1 g cm^{-3}. The calculated solubility of CO_2 and H_2S in water at 313 K, using equation 1.3, are 0.23 mol kg^{-1} and 0.60 mol kg^{-1}, respectively. The experimental data [20, 21] are 0.36 mol kg^{-1} and 0.83 mol kg^{-1}, respectively. The simulation results predict that H_2S is more soluble in water than CO_2 at the same temperature and pressure due to its higher dipole moment. The dipole moment of H_2S is closer to that of water.

The density profiles in Fig. 3-C and 3-D are for H_2O-CO_2 and H_2O-H_2S systems at 450 K. It is observed that the concentration of CO_2 is slightly larger in the liquid phase respect to that observed at 313 K. The concentration of water is 0.84 g cm^{-3}. Nevertheless, its concentration in the vapor phase is higher; this is because the molecules of CO_2 that were found at the interface at low temperature are moved to the vapor region. This produces that the concentration of CO_2 at the interface decreases considerably when the temperature increases. A similar behavior is found for H_2S, its concentration at the interface decreases when the temperature increases. The density of water decreases in both cases, as expected. The calculated solubility of CO_2 and H_2S in water at 313 K are 0.27 mol kg^{-1} and 1.26 mol kg^{-1}, respectively. The change in solubility of H_2S is much higher than that of CO_2 when the temperature varied from 313 K to 450 K.

5 Conclusions

The force fields used in this work for the acid gases give a good description of the system in the liquid phase at high pressures and temperatures. The solubility of CO_2 and H_2S in water was calculated using molecular dynamics at 313 K and 450 K. The simulation results predict that the solubility of H_2S in the liquid phase is higher than that of CO_2 at the same pressure and temperature, in agreement with experimental data. The H_2S has a dipole moment closer to that of water, that is why the molecule is more soluble. The CO_2 has not a dipole moment but it has a quadrupole. The simulation results show also that the largest adsorption of these gases is at the liquid-vapor interface. The adsorption decreases with the increase of temperature and the concentration of the acid gases increases in the vapor phase. The effect of the adsorption at the interface may be used to understand experimental results and also to test statistical mechanical theories at interfaces.

6 Acknowledgments

RLR thanks to UAM-I for a scholarship as a postgraduate student. JA thanks Conacyt for financial support.

References

1 Kamps, A. P.-S.; Balaban, A.; Jodecke, M.; Kuranov, G.; Smirnova, N. A.; Maurer, G. J. Eng. Chem. Res. 2001, 40, 696-706.
2 Jou, F. Y.; Mather, A. E.; Otto F. D. Can. J. Chem. Eng. 1995, 73, 140-147.
3 Kristof, T.; Liszi, J. J. Phys. Chem. B 1997, 101, 5480-5483.
4 Geiger, L. C.; Ladanyi, B. M.; and Chapin M. E. J. Chem. Phys. 1990, 93, 4533-4542.

5 Murthy, C. S.; Singer, K. Mol. Phys. 1981, 44, 135-143.
6 da Rocha S. R. P.; Johnston, K. P.; Westacott, R. E.; Rossky P. J. J. Phys. Chem. B 2001, 105, 12092-12104.
7 da Rocha S. R. P.; Johnston, K. P.; Rossky, P. J. J. Phys. Chem. B 2002, 106, 13250-13261.
8 Urukova, I.; Vorholz, J.; Maurer, G. J. Phys. Chem. B 2006, 110, 14943-14949.
9 Berendsen, H. J. C.; Straatsma, T. P. J. Phys. Chem. 1987, 91, 6269-6271.
10 Harris, J.; Youg, K. H. J. Phys. Chem. 1995, 99, 12021-12024.
11 Murthy, C. S.; O'Shea, S. F.; McDonald, I. R. Mol. Phys. 1983, 50, 531-541.
12 Nath, S. K. J. Phys. Chem. B 2003, 107, 9498-9504.
13 Tuckerman, M. E.; Alejandre, J.; López-Rendón, R.; Jochim, A. L.; Martyna, G. J. J. Phys. A: Math. Gen. 2006, 39, 5629-5651.
14 Martyna, G. J.; Tuckerman, M. E.; Klein, M. L. J. Chem. Phys. 1992, 97, 2635-2643.
15 Martyna, G. J.; Tobias, D. J.; Klein, M. L. J. Chem. Phys 1994, 101, 4179-4189.
16 Karasawa, N.; Goddard, III W. A. J. Phys. Chem. 1989, 93, 7320-7327.
17 Essmann, U.; Perera, L.; Berkowitz, M. L.; Darden, T.; Lee, H.; Pedersen, L. G. J. Chem. Phys 1995, 103, 8577-8593.
18 López-Lemus, J; Alejandre, J. Mol. Phys. 2002, 100, 2983-2992.
19 Lemmon, E. W.; McLinden, M. O.; Friend, D. G. Thermophysical Properties of Fluid Systems, NIST Chemistry WebBook, NIST Standard Reference Database , Eds. P.J. Linstrom and W.G. Mallard, http://webbook.nist.gov, 2005
20 Silkenbaumer, D.; Rumpf, B.; Lichtenthaler, R. N. Ind. Eng. Chem. Res. 1998, 37, 3133-3141.
21 Kuranov, G.; Rumpf, B.; Smirnova, N. A.; Maurer, G. Ind. Eng. Chem. Res. 1996, 35, 1959-1966.